Journal of Thermal Analysis and Calorimetry, Vol. 82 (2005) 373–381

THERMAL DECOMPOSITION OF LIEBIGITE
A high resolution thermogravimetric and hot-stage Raman spectroscopic study

R. L. Frost, M. L. Weier and W. Martens*

Inorganic Materials Research Program, School of Physical and Chemical Sciences, Queensland University of Technology, GPO Box 2434, Brisbane Queensland 4001, Australia

A combination of high resolution thermogravimetric analysis coupled to a gas evolution mass spectrometer has been used to study the thermal decomposition of liebigite. Water is lost in two steps at 44 and 302°C. Two mass loss steps are observed for carbon dioxide evolution at 456 and 686°C. The product of the thermal decomposition was found to be a mixture of $CaUO_4$ and Ca_3UO_6. The thermal decomposition of liebigite was followed by hot-stage Raman spectroscopy. Two Raman bands are observed in the 50°C spectrum at 3504 and 3318 cm^{-1} and shift to higher wavenumbers upon thermal treatment; no intensity remains in the bands above 300°C. Three bands assigned to the ν_1 symmetric stretching modes of the $(CO_3)^{2-}$ units are observed at 1094, 1087 and 1075 cm^{-1} in agreement with three structurally distinct $(CO_3)^{2-}$ units. At 100°C, two bands are found at 1089 and 1078 cm^{-1}. Thermogravimetric analysis is undertaken as dynamic experiment with a constant heating rate whereas the hot-stage Raman spectroscopic experiment occurs as a staged experiment. Hot stage Raman spectroscopy supports the changes in molecular structure of liebigite during the proposed stages of thermal decomposition as observed in the TG-MS experiment.

Keywords: *andersonite, dehydration, dehydroxylation, high-resolution thermogravimetric analysis, liebigite, rutherfordine, Raman spectroscopy*

Introduction

Uranium speciation is important in the safety assessment of nuclear waste repositories to predict actinide migration from such sites [1]. According to Clark *et al*. [2], actinide elements released to the environment will eventually come into contact with water, containing carbonate and/or bicarbonate anions which are exceptionally strong complexing agents for actinide ions including uranyl, $(UO_2)^{2+}$. Carbonate complexes may therefore play an important role in migration from a nuclear waste or in accidental site contamination. This is reflected also in formation of uranyl carbonate minerals such as liebigite [2]. Knowledge of conditions of formation, paragenesis and paragenetic sequences, crystal structure, thermodynamic and other properties of the uranyl minerals are therefore indispensable also from the environmental point of view. Determination of such properties can be achieved by a number of techniques. Among these techniques are the techniques of vibrational spectroscopy. Infrared and Raman spectroscopy enables an understanding not only crystal chemistry of uranyl natural and synthetic compounds, but also especially the role of water molecules and other OH groupings and hydrogen bonding in these uranyl phases. Such information is difficult to obtain by other means.

Recently, crystal structure of some uranyl tricarbonates – synthetic grimselite, $K_3Na[(UO_2)(CO_3)_3]\cdot H_2O$ [3, 4], trigonal $Na_4(UO_2)(CO_3)_3$ [4, 5], and triclinic čejkaite [6] were published. The mineral liebigite, a calcium uranyl carbonate of formula $Ca_2[UO_2(CO_3)_3]\cdot 11H_2O$ was first discovered last century [7]. Liebigite is one of the most abundant secondary uranyl carbonate mineral [8, 9]. Studies of liebigite first involved X-ray diffraction for its structure determination [8–10]. The mineral has been synthesised [11, 12]. Vochten *et al*. [12] synthesised liebigite and andersonite and studied their thermal behaviour and luminescence. Luminiscent spectrum of natural liebigite was presented also by Gorobets and Rogojine [13]. Vochten *et al*. described also the structure and physicochemical characteristics of a synthetic phase compositionally intermediate between liebigite and andersonite [14]. Gibbs free energy and enthalpy of formation of liebigite have been published [15, 16]. A theoretical study of the structure of uranyltricarbonate anion and anhydrous and hydrated liebigite have been presented [17–19].

Uranyl tricarbonates are based upon finite clusters, $(UO_2)(CO_3)_3$. This cluster is composed of a $UO_2\phi_6$ (ϕ=O^{2-}) hexagonal dipyramid that shares three equatorial edges with CO_3 triangles [20, 21]. The crystal structure of liebigite has been determined as orthorhombic system of space group Bba2-C2n17 [22, 23]. The struc-

* Author for correspondence: r.frost@qut.edu.au

1388–6150/$20.00

Akadémiai Kiadó, Budapest, Hungary
Springer, Dordrecht, The Netherlands

ture of liebigite contains these $(UO_2)(CO_3)_3$ clusters which are linked by two kinds of $CaO_4(H_2O)_4$ and one kind of $CaO_3(H_2O)_4$ polyhedron to form puckered $Ca_2UO_2(CO_3)_3{\cdot}8H_2O$ layers parallel to (001). These layers are interconnected only by hydrogen bonds, both directly as well as via three additional interlayer water molecules, two of which show positional disorder [23, 24]. Similar neutral $Ca_2UO_2(CO_3)_3$(aq.) complex was discovered in uranium mining related waters and experimentally confirmed [1, 25–31]. The infrared spectrum of liebigite has been published [32] and comparison of the infrared spectra of other uranyl carbonates made [33]. Jones and Jackson [34] included the infrared spectrum of liebigite without any interpretation in their atlas of the infrared transmission spectra of carbonate minerals. Amayri [31] shortly discussed infrared and Raman spectra of synthetic liebigite.

The number of thermoanalytical studies of minerals such as liebigite are very few [35–38]. Čejka and Urbanec reported the DTA analysis of liebigite [37]. Endotherms were found at 105 and 480°C and were attributed to dehydration and partial decarbonation. Thermogravimetry showed the loss of water occurred in steps. Čejka and Urbanec found that 6 moles of water were lost between ambient and 100°C, 3.5 moles in the range 100 to 200°C and 1.5 moles in the range 200 to 300°C [37]. Decarbonation was also found to take place in steps although some uncertainty existed as to the number of steps. Thermal analysis has been shown to be useful for the study of the thermal decomposition of complex mineral systems [39–43]. In this work we undertake the thermal analysis of liebigite using thermogravimetry coupled to a mass spectrometer. This information is complimented with hot stage Raman spectroscopy.

Experimental

Minerals

The mineral liebigite was obtained from Mineralogical Research Company, California. Sample collected from Schwartzwalder Mine, Near Golden, Jefferson County, Colorado. The mineral was analysed by X-ray diffraction for phase purity and by electron probe using energy dispersive techniques for quantitative chemical composition. The mineral was found to be phase pure.

X-ray diffraction

X-ray diffraction (XRD) patterns were recorded using CuK_α radiation (n=1.5418 Å) on a Philips PANalytical X' Pert PRO diffractometer operating at 40 kV and 40 mA with 0.125° divergence slit, 0.25° anti-scatter slit, between 3 and 15° (2θ) at a step size of 0.0167°. For low angle XRD, patterns were recorded between 1 and 5° (2θ) at a step size of 0.0167° with variable divergence slit and 0.5° anti-scatter slit.

Thermal analysis

Thermal decomposition of the liebigite was carried out in a TA® Instruments incorporated high-resolution thermogravimetric analyzer (series Q500) in a flowing nitrogen atmosphere (80 cm^3 min^{-1}). 34.4 mg of sample underwent thermal analysis, with a heating rate of 5°C min^{-1}, resolution of 6 to 1000°C. With the quasi-isothermal, quasi-isobaric heating program of the instrument the furnace temperature was regulated precisely to provide a uniform rate of decomposition in the main decomposition stage. The TG instrument was coupled to a Balzers (Pfeiffer) mass spectrometer for gas analysis. Only water vapour, carbon dioxide and oxygen were analyzed.

Hot stage Raman microprobe spectroscopy

The crystals of liebigite were placed and oriented on the stage of an Olympus BHSM microscope, equipped with 10× and 50× objectives and part of a Renishaw 1000 Raman microscope system, which also includes a monochromator, a filter system and a Charge Coupled Device (CCD). Raman spectra were excited by a HeNe laser (632.8 nm) at a resolution of 2 cm^{-1} in the range between 100 and 4000 cm^{-1}. Repeated acquisition using the highest magnification was accumulated to improve the signal to noise ratio. Spectra were calibrated using the 520.5 cm^{-1} line of a silicon wafer. In order to ensure that the correct spectra are obtained, the incident excitation radiation was scrambled. Previous studies by the authors provide more details of the experimental technique [44–47]. Spectra at elevated temperatures were obtained using a Linkam thermal stage (Scientific Instruments Ltd, Waterfield, Surrey, England). Details of the technique have been published by the authors [48–53]. Spectral manipulation such as baseline adjustment, smoothing and normalisation was performed using the GRAMS® software package (Galactic Industries Corporation, Salem, NH, USA).

Results and discussion

High resolution thermogravimetric analysis and mass spectrometric analysis

The thermogravimetric analysis of liebigite over the ambient to 1000°C temperature range is shown in Fig. 1 and the mass spectra as measured by the relative ion current for water and carbon dioxide in Fig. 2. The mass gain of the evolved water vapour shows two steps at

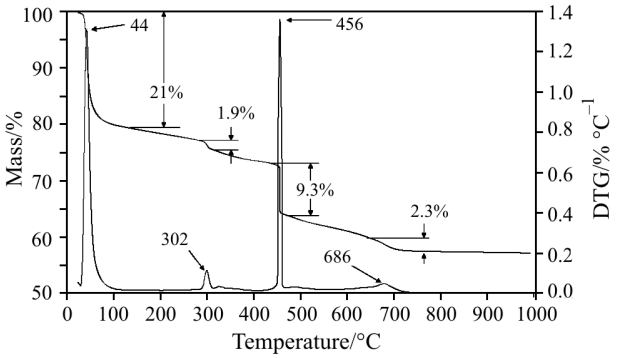

Fig. 1 TG and DTG of liebigite

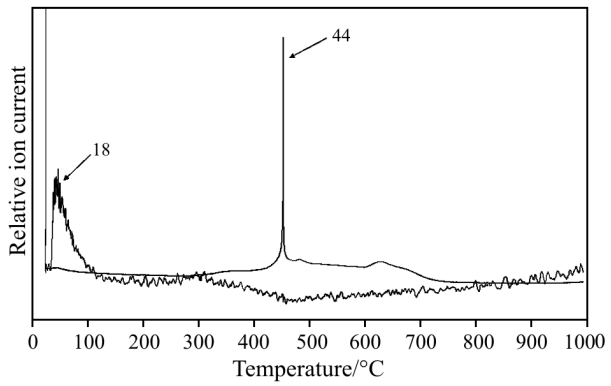

Fig. 2 Ion current-temperature plot for liebigite

around 44 and at 302°C. The experimentally determined mass loss of water is 27.0%. This corresponds precisely to the theoretical mass loss of water based upon the formula for liebigite of ($Ca_2[UO_2(CO_3)_3]\cdot 11H_2O$). The mass loss at 44°C is 21.1% which corresponds to 9 moles of water. The remainder of the water (5.9%) is lost at 302°C. This corresponds to 2 moles of water. Such a result is in harmony with the results of Čejka and Urbanec who inferred three mass loss steps of 6, 3.5 and 1.5 moles of water [37]. Two mass loss steps are observed for carbon dioxide at 456 and 686°C. The total mass loss of carbon dioxide is 15.9 % which is less than the predicted value of 18.1%.

X-ray diffraction

The XRD patterns of the liebigite before and after thermal analysis are shown in Fig. 3. XRD pattern of sample was matched by liebigite pattern 01-075-1705. The XRD patterns confirm the sample is liebigite. Following heat treatment the XRD pattern of the thermally treated liebigite was matched by a combination of calcium uranium oxide patterns 01-085-0577 and 01-071-2199. The result of the analysis shows that the thermally treated liebigite is a mixture of $CaUO_4$ and Ca_3UO_6.

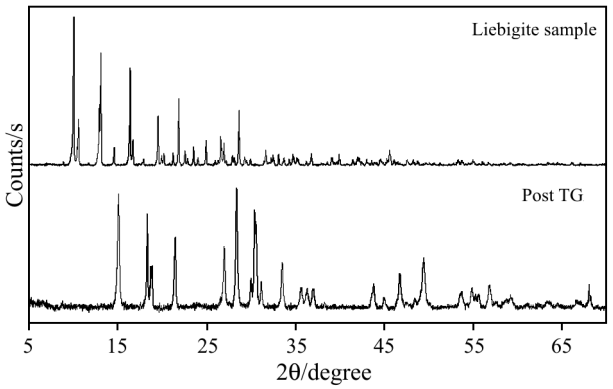

Fig. 3 X-ray diffraction patterns of liebigite before and after thermal treatment

Stages of the thermal decomposition of liebigite

The following steps are proposed for the thermal decomposition of liebigite:

- Step 1 at 44°C

$$Ca_2[UO_2(CO_3)_3]\cdot 11H_2O \rightarrow$$
$$\rightarrow Ca_2[UO_2(CO_3)_3]\cdot 2H_2O + 9H_2O$$

- Step 2 at 302°C

$$Ca_2[UO_2(CO_3)_3]\cdot 2H_2O \rightarrow Ca_2[UO_2(CO_3)_3] + 2H_2O$$

- Step 3 at 456°C

$$Ca_2[UO_2(CO_3)_3] \rightarrow Ca_2UO_5 + 3CO_2$$

$$2Ca_2UO_5 \rightarrow CaUO_4 + Ca_3UO_6$$

The mechanism for the thermal decomposition of liebigite is based upon the dehydration of the mineral in two steps followed by the decarbonation in two steps resulting in the formation of two calcium uranate minerals. These results differ from that of Čejka and Urbanec who proposed the decarbonation of liebigite in multiple steps [37]. The end products in this work are in agreement with these workers.

Hot stage Raman spectroscopy of liebigite

The hot stage Raman spectroscopy using the Linkham thermal stage is a stepwise process in which the mineral is heated to a pre-selected temperature, with a wait time to ensure constant temperature then the spectra are collected before the sample is heated to the next pre-selected temperature. In contrast the TG experiment is a dynamic experiment in which the sample is heated at a constant rate. Therefore the chemical changes as determined by the hot-stage Raman spectroscopy may not exactly match the mass loss changes of the TG experiment.

The free linear uranyl group, $(UO_2)^{2+}$, symmetry $D_{\infty h}$, has four normal vibrations but three fundamental

bands only: ν_1 (approximately 900–700 cm^{-1}) – the symmetric stretching fundamental, only Raman active; $\nu_2(\delta)$ (approximately 260–180 cm^{-1}) – the doubly degenerate bending fundamental, only IR-active; ν_3 (approximately 1000–850 cm^{-1}) – the antisymmetric stretching fundamental, only IR active. Distortion of the uranyl group or change in the local symmetry can result in the removal of the degeneracy and Raman activation of the ν_2 mode and IR activation of the ν_1 mode. The carbonate ion of D_{3h} symmetry has four fundamentals: ν_1 (approximately 1115–1050 cm^{-1}) – the symmetric stretching vibration; ν_2 (aproximately 880–835 cm^{-1}) – the out-of-plane bending vibration; ν_3 (approximately 1610–1250 cm^{-1}) – the doubly degenerate stretching vibration; ν_4 (approximately 770–670 cm^{-1}) – the doubly degenerate in-plane bending vibration. In $(UO_2)(CO_3)_3$ the carbonate clusters may remain planar, but owing to the bidentate coordination their symmetry is lowered from D_{3h} to C_{2v} or lower. Consequently each of the two doubly degenerate modes splits into two bands leading to a total number of six IR and Raman active vibrations. The number of observed bands assigned to the carbonate vibrations in the infrared and Raman spectra of liebigite studied indicates the symmetry decrease of carbonate ions from D_{3h} to C_{2v} or lower. This causes activation of all vibrations, the ν_1 symmetric stretching, the ν_2 symmetric bending, the ν_3 antisymmetric stretching, and the ν_4 antisymmetric bending vibrations in IR and Raman spectra, and splitting of the doubly degenerate ν_2 and the triply degenerate ν_3 and ν_4 vibrations.

Raman spectroscopy of the hydroxyl stretching region using the thermal stage

The Raman spectra of the hydroxyl stretching region of liebigite as a function of temperature are shown in Fig. 4. The sharp feature at around 2880 cm^{-1} is due to cosmic radiation and is not part of the spectral results. Two Raman bands are observed in the 50°C spectrum at 3504 and 3318 cm^{-1}. These bands are observed in the 25°C spectra at 3498 and 3299 cm^{-1}. The bands shift to higher wavenumbers upon thermal treatment of the liebigite and no intensity remains in the bands above 300°C. Such an observation is in excellent agreement with the TG results which show that in the second TG step all the water has been removed from the liebigite sample. The observation of two Raman bands with different wavenumbers is attributed to two different non-equivalent water molecules in the liebigite structure. The difference in the wavenumbers of the two bands indicates a difference in hydrogen bonding of the two water molecules. The changes in the position of the bands with temperature increase indicate changes in the hydrogen bonding of the water in the liebigite structure. The shift in band position is an indication of change in hydrogen bond length. At 300°C only a single band is observed at 3550 cm^{-1} showing that at this temperature only one type of water molecule is observed. The second water molecule is gradually removed before reaching 300°C. The variation in the band position as a function of temperature is illustrated in Fig. 5.

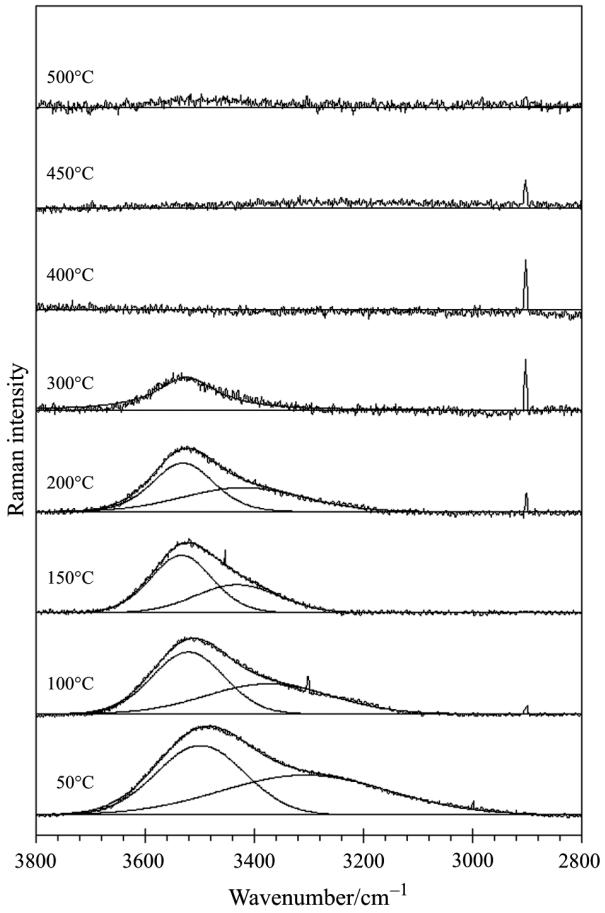

Fig. 4 Raman spectra of the hydroxyl stretching region of liebigite over the 50 to 500°C temperature range

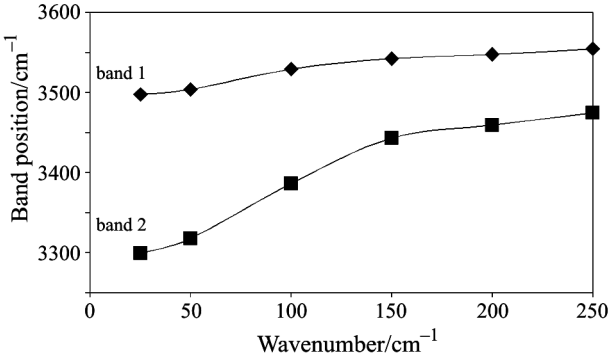

Fig. 5 Variation in the band positions of the hydroxyl stretching vibrations as a function of temperature

Raman spectroscopy of the $(CO_3)^{2-}$ stretching region as a function of temperature

The Raman spectra in the 600 to 1200 cm^{-1} region of thermally treated liebigite are shown in Fig. 6. In these spectra there are three distinct regions (a) the 1050 to 1150 cm^{-1} region attributed to the $(CO_3)^{2-}$ symmetric stretching vibrations, (b) the 800 to 900 cm^{-1} region ascribed to the ν_2 bending modes and (c) 700 to 800 cm^{-1} region assigned to the symmetric stretching modes of the $(UO_2)^{2+}$ units. Three bands are observed in the spectra of the $(CO_3)^{2-}$ units of liebigite around 1100 cm^{-1} in the 50°C spectrum at 1094, 1087 and 1075 cm^{-1}. In liebigite there are three structurally distinct $(CO_3)^{2-}$ units and as a consequence more than one symmetric stretching mode may be predicted. In the 100°C spectrum two bands are found at 1089 and 1078 cm^{-1}. These bands are assigned to the ν_1 symmetric stretching modes of the $(CO_3)^{2-}$ units. The observation of two bands suggests two distinct $(CO_3)^{2-}$ units in the crystal structure of liebigite above 100°C. The intensity of these bands remains constant up to 400°C after which the intensity decreases significantly with temperature. At 500°C almost no intensity remains in this spectral region.

The Raman spectra of liebigite as a function of temperature in the region from 1200 to 1800 cm^{-1} are shown in Fig. 7. This spectral region contains the doubly degenerate antisymmetric stretching $(CO_3)^{2-}$ vibrations together with δH_2O bending modes [54]. A band is observed in the Raman spectra at around 1690 cm^{-1}. This band is attributed to the water bending vibration. The intensity of the band decreases with increasing temperature and a comparison may be made with the decrease in intensity of the bands assigned to the water stretching vibrations (Fig. 4). The intensity of both the water bending mode and the OH stretching vibration are lost above 300°C.

A relatively broad band is observed at around 1630 cm^{-1} (Fig. 7). The position of the band decreases with increasing temperature. This band is assigned to the water bending mode. The broadness of the band is associated with the different hydrogen bonding.

Two bands are observed in the 50°C Raman spectrum of liebigite at 1403 and 1370 cm^{-1} and are assigned to the ν_3 antisymmetric stretching vibrations. In the in-

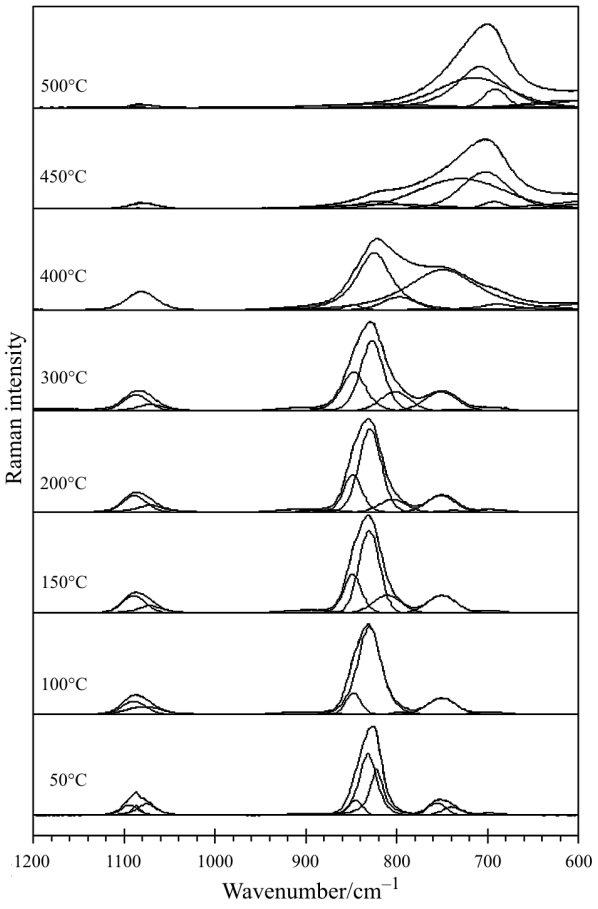

Fig. 6 Raman spectra of the 600–1200 cm^{-1} region of liebigite over the 50 to 500°C temperature range

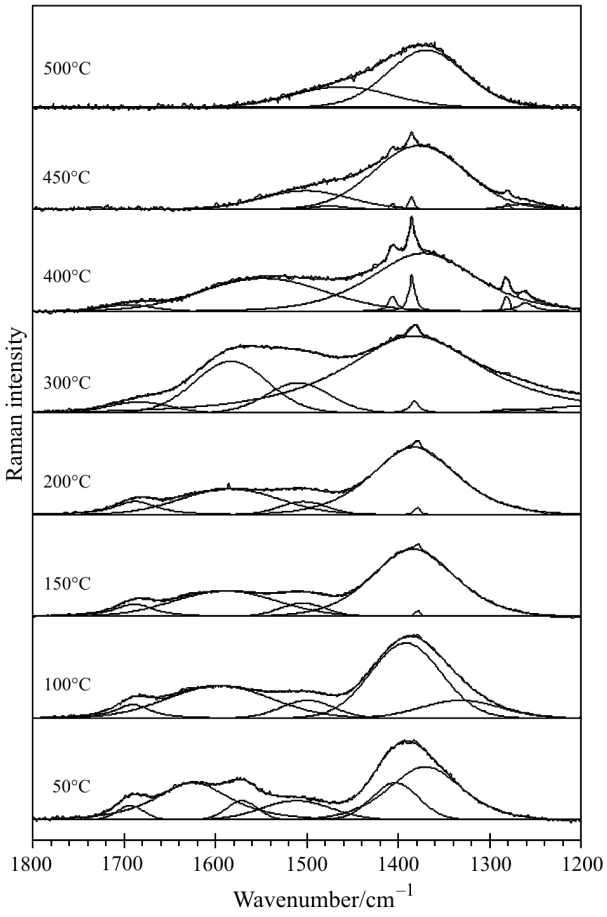

Fig. 7 Raman spectra of the 1200–1800 cm^{-1} region of liebigite over the 50 to 500°C temperature range

frared spectrum three overlapping bands are observed at 1451, 1400 and 1380 cm^{-1}. Čejka reported three infrared bands at 1590, 1538 and 1378 cm^{-1} attributed to the $\nu_3(CO_3)^{2-}$ antisymmetric stretching vibrations, and that at 1632 cm^{-1} to the δH_2O bending vibration [33]. Amayri [54] published infrared spectra of synthetic bayleyite, liebigite, $Sr_2(UO_2)(CO_3)_3 \cdot 8H_2O$, and $Ba_2(UO_2)(CO_3)_3 \cdot 6H_2O$ and observed bands at 1379.3, 1512.7, 1546.9, 1627 cm^{-1} (bayleyite), 1384.8, 1404.3, 1537, and 1620 cm^{-1} (liebigite), 1346.5, 1384.4, 1545, 1564.9 and 1616.5 cm^{-1} (Sr uranyl tricarbonate), and 1379.5, 1517.0, 1544.8 and 1616.5 cm^{-1} (Ba uranyl tricarbonate). Amayri assigned bands in the range 1300–1565 cm^{-1} to the ν_3 $(CO_3)^{2-}$ antisymmetric stretching vibration, while those in 1615–1630 cm^{-1} to the δH_2O bending vibration [54]. A sharp band at 1378.5 cm^{-1} appears to increase in intensity with temperature increase. At 400°C two bands are observed at 1385 and 1406 cm^{-1}. These bands are attributed to the formation of a calcium carbonate. This phase may be an intermediate in the decomposition of liebigite. At higher temperatures this phase is lost.

Raman spectroscopy of the UO_2 stretching region as a function of temperature

One of the difficulties in studying the Raman (and infrared) spectra of uranyl carbonates is the potential overlap of bands associated with $(UO_2)^{2+}$ and the $(CO_3)^{2-}$ units. The region for the symmetric stretching vibration of the $(CO_3)^{2-}$ units is a spectral window free from bands ascribed to the $(UO_2)^{2+}$ units. One potential overlap is between the antisymmetric stretching vibrations of the $(CO_3)^{2-}$ units and the δ water modes. Another major difficulty is the possible overlap of the symmetric stretching modes of the $(UO_2)^{2+}$ units and the bending modes of the $(CO_3)^{2-}$ units. There is another consideration caused by the presence or absence of water in the structure. The presence of water may cause significant shifts in the bands associated with both $(UO_2)^{2+}$ units and $(CO_3)^{2-}$ units.

The spectra of the symmetric stretching region of the $(UO_2)^{2+}$ units are shown in Fig. 6. The overlap of the bending modes of the $(CO_3)^{2-}$ units can also occur in is observed in Fig. 6. The band observed at 831 cm^{-1} is assigned to this mode and may be resolved into three components at 845, 831 and 822 cm^{-1}. The intensity of these bands remains constant up to 400°C but as thermal decomposition occurs the intensity of these bands approaches zero. This would thus indicate that the bands centred upon 755 cm^{-1} are attributed to the symmetric stretching modes of the $(UO_2)^{2+}$ units. The intensity of bands in this region increases with temperature increase.

Raman spectroscopy of the CO_3 bending region as a function of temperature

An intense band is observed at 822 cm^{-1} for liebigite and is attributed to the ν_2 bending modes of the $(CO_3)^{2-}$ units (Fig. 6). The band is not observed in the infrared spectrum although a low intensity band at 820 cm^{-1} is found. One possible assignment is that the band at 822 cm^{-1} is due to the symmetric stretching modes of the $(UO_2)^{2+}$ units and the band at 823 cm^{-1} to the ν_2 bending modes of the $(CO_3)^{2-}$ units. It is not known whether the bands at around 823 cm^{-1} are due to the ν_1 symmetric stretching mode of the $(UO_2)^{2+}$ units or the out of plane ν_2 bending modes of the $(CO_3)^{2-}$ units. It is probable that both bands overlap or occur at the same wavenumber. Calculated range $[\nu_1(UO_2)^{2+}=0.94\nu_3(UO_2)^{2+}$ cm^{-1}, and $\nu_1(UO_2)^{2+}=0.89\nu_3(UO_2)^{2+}+21$ cm^{-1} [33] corresponds approximately to 798–848 cm^{-1}. A band in the 800 to 830 cm^{-1} has been previously observed in the Raman spectra and has been attributed to the ν_1 band of the $(UO_2)^{2+}$ units [55]. Amayri assigned the band at 826 cm^{-1} (Raman) to the $\nu_1(UO_2)^{2+}$ [54]. Such an assignment is open to question because of the obvious overlap of the two vibrations as mentioned above. Čejka reported the stretching vibrations of the $(UO_2)^{2+}$ units for a number of calcium uranate minerals based upon infrared measurements [56]. The band position for the symmetric stretching $(UO_2)^{2+}$ vibration for a range of synthetic uranyl tricarbonates varied from between 808 and 831 cm^{-1}.

For the mineral andersonite Čejka *et al*. assigned a band at 795 cm^{-1} to the ν_1 band of the $(UO_2)^{2+}$ units [57], but, on the contrary Wilkins attributed a band at 836 cm^{-1} (Raman) to this vibration [58]. One may assume that in both liebigite samples studied, observed bands related to the $\nu_1(UO_2)^{2+}$ may be approximately located in the range 848–798 and 835–807 cm^{-1}, respectively, as calculated from the wavenumbers of the $\nu_3(UO_2)^{2+}$ vibrations. This corresponds to the U–O bond lengths in uranyl 1.7732–1.7946 and 1.7684–1.8139 Å, respectively. This agrees with 1.784(7) and 1.774(7) Å from the Mereiter's crystal structure analysis and EXAFS data 1.80–1.81 Å for synthetic liebigite [54]. Some of these bands may be attributed to the ν_1 symmetric stretching modes of the $(UO_2)^{2+}$ units, and the other to the $\nu_2(CO_3)^{2-}$ bending vibration. Such a vibration should be inactive if the symmetry of the $(UO_2)^{2+}$ units is D_{2h}; however symmetry lowering may activate the mode if the symmetry is C_s. Separation of uranyl symmetric stretching vibrations and carbonate out-of plane bending vibrations in this region is very difficult.

Bands at around 750 cm^{-1} may be ascribed to the ν_4 in-plane bending region of the $(CO_3)^{2-}$ units. Two bands for liebigite are observed at 755 and 739 cm^{-1} of about equal intensity and are assigned to this vibration. A single intense infrared band is observed at 739 cm^{-1}

and is ascribed to this mode. In the infrared spectrum two bands are found at 745 and 730 cm^{-1}. Čejka reported bands at 742, 737 and 682 cm^{-1} for the ν_4 in-plane bending modes of liebigite [33]. Amayri attributed bands at 744 and 692 cm^{-1} in the infrared spectrum and that at 756.39 cm^{-1} in the Raman spectrum of synthetic liebigite to this vibration [54]. The observation of multiple bands is attributed to the non-equivalence of the carbonate units in the liebigite structure. Recent XAFS studies also showed the non-equivalence of the carbonate units in uranyl carbonates [59]. Such studies are important for the speciation of uranyl compounds in environmental situations [60, 61].

Thermal treatment of the liebigite results is considerable changes in this spectral region. Whilst two bands are observed at 755 and 739 cm^{-1} in the 25°C spectrum, only a single band is found at 750 cm^{-1} at 50°C. This band remains unchanged up to 350°C. The 400°C spectrum is very different and a broad band at 749 cm^{-1} is observed. In the 450°C spectrum two bands are found at 702 and 729 cm^{-1}. The bands are found at 708 and 715 cm^{-1} in the 500°C spectrum. Since there is no water or carbonate remaining in the thermally treated sample, these bands must be attributed to UO vibrations. These bands must correspond to the uranium oxide as determined by the X-ray diffraction.

Raman spectroscopy of the UO_2 bending region as a function of temperature

The Raman spectra of the low wavenumber region of liebigite are shown in Fig. 8. A single intense band is observed for liebigite sample m31082 at 248 cm^{-1} and is assigned to the ν_2 bending modes of the $(UO_2)^{2+}$ units. Čejka based upon farIR spectra suggested that the ν_2 bending modes occurred at 286 or 316 or 280 cm^{-1} [33]. One of the advantages of Raman spectroscopy is the ability to obtain spectral data in the low wavenumber region. The low wavenumber region of liebigite sample is complex. An intense band is found at 246 cm^{-1} and is assigned to the ν_2 bending modes of the $(UO_2)^{2+}$ units. A second intense band is observed at 201 cm^{-1}. The band at 246 cm^{-1} appears to shift towards 234 cm^{-1} at 100°C and to 231 cm^{-1} as the temperature is increased. The band also increases in intensity with temperature increase. The spectral profile is similar in the spectra up to 300°C. Additional bands are observed in the 400, 500 and 600°C spectra. An intense band is observed with increasing intensity at around 525 cm^{-1}. Čejka suggested that a possible coincidence of ν_2 $\delta(UO_2)^{2+}$ and UO ligand vibrations [33]. In the infrared and Raman spectra of $K_4(UO_2)(CO_3)_3$, Anderson *et al*. [16] ascribed bands in the range 241–307 cm^{-1} to the $(UO_2)^{2+}$ to the $\delta(UO_2)^{2+}$ bending vibrations and those in the range 152–211 cm^{-1} to the $(CO_3)^{2-}$ librations.

Raman spectroscopy in harmony with the results of the TG-MS

Raman spectroscopy enables the molecular structure of the liebigite mineral to be obtained as a function of temperature. Hot stage Raman spectroscopy enables the molecular structure of the liebigite to be obtained in situ at the elevated temperature. Raman spectroscopy of the thermally treated liebigite fits well with the TG-MS results. TG shows the loss of water at 302°C. Raman spectroscopy shows a decrease in intensity of the water OH stretching region up to 300°C after which no intensity remains. TG-MS shows that water is lost at low temperatures around 44°C. The Raman spectra show a steady loss of water up to 100°C. The TG-MS experiment shows a loss of carbon dioxide at 456°C. The Raman spectra shows more than one species of carbonate present in the 50 to 300°C temperature range. Above this temperature only one carbonate band is observed. The intensity of this band approaches zero by 450°C. This confirms the loss of carbonate from the mineral as determined by the thermogravimetric experiment. The band at 831 cm^{-1} assigned to the carbonate bending mode decreases in intensity with thermal

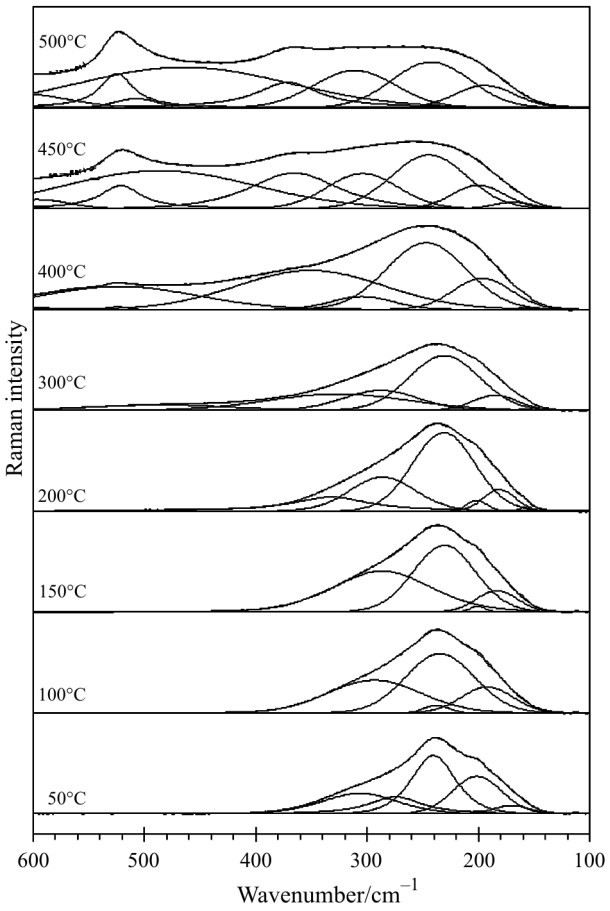

Fig. 8 Raman spectra of the 100–600 cm^{-1} region of liebigite over the 50 to 500°C temperature range

treatment in harmony with the stretching vibration centred on 1087 cm^{-1}. The second band at 829 cm^{-1} in the 50°C spectrum decreases in band position to 824 cm^{-1} at 400°C. Above 400°C the bands show no intensity and additional bands are observed at 702 and 729 cm^{-1}.

It must be kept in mind that the TG-MS is a dynamic experiment in which the liebigite is heated at a constant rate even though the rate might be quite slow. The Raman spectroscopic experiment is a 'batch' type experiment in which the sample is heated to a specific temperature held at that temperature before being heated to the next selected temperature. Thus the results of the hot stage Raman experiment may not be precisely the same as that from the TG-MS experiment.

Conclusions

The thermal decomposition of the mineral liebigite, a natural calcium uranyl tricarbonate, has been followed by a combination of thermogravimetry coupled to a mass spectrometer and hot stage Raman spectroscopy. The phase identification of the mineral was shown using XRD techniques to be liebigite and the products of the thermal decomposition confirmed. The water in liebigite is released in two steps (a) at low temperatures around 44 and at (b) 302°C. The decarbonation takes place at 456 and 686°C.

The mineral liebigite is an interesting mineral because of its structure with 8 formula units per unit cell and with non-equivalent carbonate and non-equivalent UO bonds. Raman spectroscopy confirms the non-equivalence of both units by the observation of additional bands for the $(CO_3)^{2-}$ units and UO_2 units. Three symmetric stretching modes of the $(CO_3)^{2-}$ units are observed confirming the presence of three non-equivalent carbonates. This non-equivalence is translated into the antisymmetric stretching region where multiple ν_3 stretching vibrations are observed.

Acknowledgements

The financial and infra-structure support of the Queensland University of Technology Inorganic Materials Research Program of the School of Physical and Chemical Sciences is gratefully acknowledged. The Australian Research Council (ARC) is thanked for funding.

The authors wish to thank and gratefully acknowledge the support of Mr Dermot Henry of Museum Victoria for the loan of the minerals used in this study.

References

1 S. N. Kalmykov and G. R. Choppin, Radiochim. Acta, 88 (2000) 603.
2 D. L. Clark, D. E. Hobart and M. P. Neu, Chem. Revs., 95 (1995) 25.
3 Y. Li and P. C. Burns, Can. Mineral., 39 (2001) 1147.
4 Y. Li, S. V. Krivovichev and P. C. Burns, Mineralogical Magazine, 65 (2001) 297.
5 I. Císarová, R. Skála, P. Ondruš and M. Drábek, Acta Cristallogr. Sect. E, Struct. Rep. Online, E57 (2001) i32.
6 P. Ondruš, R. Skála, F. Veselovský, J. Sejkora and C. Vitti, Am. Mineral., 88 (2003) 686.
7 E. S. Larsen, Am. Mineral., 2 (1917) 87.
8 C. Frondel, Am. Mineral., 35 (1950) 245.
9 H. T. Evans, Jr. and C. Frondel, Am. Mineral., 35 (1950) 251.
10 H. Neumann and K. O. Bryn, Avhandl. Norske Videnskaps-Akad. Oslo., I., Mat.-Naturv. Kl., (1958), p. 6.
11 R. Meyrowitz, D. R. Ross and A. D. Weeks, U.S. Geological Survey Professional Paper, 475-B (1963) 162.
12 R. Vochten, L. Van Haverbeke and K. Van Springel, Can. Mineral., 31 (1993) 167.
13 B. S. Gorobets and A. A. Rogojine, All-Russia Institute of Mineral Resources, Moscow 2002.
14 R. Vochten, L. Van Haverbeke, K. Van Springel, N. Blaton and O. M. Peeters, Can. Mineral., 32 (1994) 553.
15 A. K. Alwan and P. A. Williams, Mineralogical Magazine, 43 (1980) 665.
16 F. Chen, R. C. Ewing and S. B. Clark, Am. Mineral., 84 (1999) 1208.
17 P. Pyykkö, J. Li and N. Runeberg, J. Phys. Chem., 98 (1994) 4809.
18 L. Gagliardi, I. Grenthe and B. O. Roos, Inorg. Chem., 40 (2001) 2976.
19 S. Tsushima, Y. Uchida and T. Reich, Chem. Phys. Lett., 357 (2002) 73.
20 P. C. Burns, M. L. Miller and R. C. Ewing, Can. Mineral., 34 (1996) 845.
21 P. C. Burns, Rev. Mineralogy, 38 (1999) 23.
22 S. Amayri, G. Geipel, W. Matz, G. Schuster, L. Baraniak, G. Bernhard and H. Nitsche, Inst. Radiochem., Forschungszentrum Rossendorf e.V., FIELD URL, Dresden, Germany 1998, p. 14.
23 K. Mereiter, TMPM, Tschermaks Mineralogische und Petrographische Mitteilungen, 30 (1983) 277.
24 K. Mereiter, Neues Jahrbuch für Mineralogie, Monatshefte, 1986, p. 325.
25 G. Bernhard, V. Brendler, G. Geipel and H. Nitsche, Freiberger Isotopenkolloquium, Proceedings, Freiberg, Germany, Sept. 30–Oct. 2, 1996 (1996) 19.
26 G. Geipel, A. Brachmann, V. Brendler, G. Bernhard and H. Nitsche, Radiochim. Acta, 75 (1996) 199.
27 G. Bernhard, G. Geipel, V. Brendler and H. Nitsche, Radiochim. Acta, 74 (1996) 87.
28 G. Bernhard, G. Geipel, V. Brendler and H. Nitsche, Inst. Radiochem., Forschungszent. Rossendorf e.V., Dresden, Germany 1996, p. 1.
29 G. Bernhard, G. Geipel, T. Reich, V. Brendler, S. Amayri and H. Nitsche, Radiochim. Acta, 89 (2001) 511.
30 G. Geipel, G. Bernhard and V. Brendler, Uranium in the Aquatic Environment, Proceedings of the International Conference [on] Uranium Mining and Hydrogeology III and the International Mine Water Association Symposium, Freiberg, Germany, Sept. 15–21, 2002 (2002) 369.

31 S. Amayri, Thesis, Fakultät Mathematik und Naturwissenschaften der Technischen Universität Dresden, Wissenschaftlich-Technischer Bericht FZR-359, 2002, p. 168, Institut für Radiochemie, Forschungszentrum Rossendorf, Germany 2002.
32 Z. Urbanec and J. Čejka, Casopis Narodniho Muzea v Praze, Rada Prirodovedna, 148 (1979) 16.
33 J. Čejka, Rev. Mineralogy, 38 (1999).
34 G. C. Jones and B. Jackson, Infared transmission spectra of carbonate minerals, Chapman and Hall, London 1993.
35 J. Čejka, K. Tobola and Z. Urbanec, Proc. Eur. Symp. Therm. Anal., 1 (1976) 353.
36 J. Čejka, K. Tobola and Z. Urbanec, J. Thermal Anal., 12 (1977) 117.
37 J. Čejka and Z. Urbanec, Casopis Narodniho Muzea v Praze, Rada Prirodovedna, 148 (1979) 177.
38 J. Čejka and Z. Urbanec, Casopis Narodniho Muzea v Praze, Rada Prirodovedna, 146 (1979) 114.
39 E. Horváth, J. Kristóf, R. L. Frost, N. Heider and V. Vagvölgyi, J. Therm. Anal. Cal., 78 (2004) 687.
40 R. L. Frost and K. L. Erickson, J. Therm. Anal. Cal., 78 (2004) 367.
41 Y. Xi, Z. Ding, H. He and R. L. Frost, J. Colloid Interface Sci., 277 (2004) 116.
42 Z. Ding and R. L. Frost, Thermochim. Acta, 416 (2004) 11.
43 R. L. Frost, M. L. Weier and K. L. Erickson, J. Therm. Anal. Cal., 76 (2004) 1025.
44 R. L. Frost and M. L. Weier, Thermochim. Acta, 406 (2003) 221.
45 R. L. Frost and Z. Ding, Thermochim. Acta, 405 (2003) 207.
46 E. Horváth, R. L. Frost, E. Makó, J. Kristóf and T. Cseh, Thermochim. Acta, 404 (2003) 227.
47 R. L. Frost, M. L. Weier, W. Martens, J. T. Kloprogge and Z. Ding, Thermochim. Acta, 403 (2003) 237.
48 R. L. Frost, T. Kloprogge, M. L. Weier, W. N. Martens, Z. Ding and H. G. H. Edwards, Spectrochim. Acta, Part A, 59 (2003) 2241.
49 R. L. Frost, M. Crane, P. A. Williams and J. T. Kloprogge, J. Raman Spectrosc., 34 (2003) 214.
50 R. L. Frost, Spectrochim. Acta, Part A 59A (2003) 1195.
51 W. Martens, R. L. Frost and J. T. Kloprogge, J. Raman Spectrosc., 34 (2003) 90.
52 W. Martens, R. L. Frost and P. A. Williams, J. Raman Spectrosc., 34 (2003) 104.
53 W. N. Martens, R. L. Frost, J. T. Kloprogge and P. A. Williams, Am. Mineral., 88 (2003) 501.
54 S. Amayri, in i-xiv, Germany 2002, p. 1.
55 A. Anderson, C. Chieh, D. E. Irish and J. P. K. Tong, Can. J. Chem., 58 (1980) 1651.
56 J. Čejka, Rev. Mineralogy, 38 (1999) 521.
57 J. Čejka, Z. Urbanec and J. Čejka, Jr., Neues Jahrbuch fuer Mineralogie, Monatshefte, 1987, p. 488.
58 R. W. T. Wilkins, Neues Jahrbuch für Mineralogie, Abhandlungen, 10 (1971) 440.
59 J. G. Catalano and G. E. Brown, Jr., Am. Mineral., 89 (2004) 1004.
60 G. Catalano Jeffrey, M. Heald Steven, M. Zachara John and E. Brown Gordon, Jr., Environ. Sci. Technol., 38 (2004) 2822.
61 J. G. Catalano, S. M. Heald, J. M. Zachara and G. E. Brown, Jr., Environ. Sci. Technol., 38 (2004) 2822.

Received: February 22, 2005
In revised form: April 11, 2005

DOI: 10.1007/s10973-005-6847-9